Proceedings of the 1999 IEEE
International Workshop on Robot and Human Interaction
Pisa, Italy – September 1999

A 7 dof pneumatic Muscle Actuator (pMA) powered Exoskeleton

N.Tsagarakis, D.G.Caldwell and G.A.Medrano-Cerda
Dept. Of Electronic Eng.
University of Salford, Salford, M5 4WT, UK

Abstract

The development of haptic systems for VR and telepresence has been identified as a key feature in the progression from observation of the environment to interaction. Arm masters and exoskeletons have formed an important user interface for the provision of such facilities, with these devices requiring a subtly combination of complex mechanical, electrical and kinematic structures with user requirements of low mass, portability, comfort, flexibility and safety. The actuation system is often identified as a focus of this design blending process.

This work considers the design, construction and testing of a light weight comfortable high power 7 degree of freedom force feedback exoskeleton. This is achieved through the use, modeling and control of pneumatic Muscle Actuators (pMA) that provide lightweight, low cost, flexible, portable, comfortable and inherently safe input/feedback/control operation. Models of operation in a virtual environment are developed and demonstrated, with experimental results to illustrate the effectiveness of the device in replicating contact forces and creating a sensation of virtual presence.

INTRODUCTION

Advances in VR and telepresence and the development and projected developments in tele/virtual medicine, tele/virtual training and high performance control of telepresence robotics for operation in hazardous environments, have highlighted the need for more effective human-computer interfaces [1]. Within this environment the major thrust has been the production of effective and realistic visual and audio effects, but a vital third component of the virtual and remote (telepresence) world is the sensation of contact. This ability to physically **interact** with remote/virtual objects rather than simply observing them has been identified as a key gap area in the generic technology for the exploitation of VR/telepresence [2] and this has simulated research activity into a variety of broadly based haptic systems ranging from desk, floor and ceiling grounded devices , to hand masters (for position detection and force feedback) and tactile feedback gloves (for pressure, texture, temperature) [3].

However, of all the haptic devices the most common are the bi-lateral master/slaves developed initially for nuclear applications. Although these devices can have excellent performance and have a long developmental history, they do have limitations for potential employment as general purpose input devices for VR and mass application telepresence systems [4]:

i). The systems are highly engineered and costly;
ii). Master and slave are solidly mounted and not portable;
iii). The master is heavy although with gravity and force compensation the operator need not be aware of the mass;
iv). To become proficient may require considerable training;
v). Most systems are driven by electrical motors often with considerable gearing and pose a potential crush/pinning danger.
vi). The mechanisms are generally for robotic applications and designs seldom have human shoulder - upper limb kinematics, preventing their easy application to VR training/control scenarios.

To reduce or overcome these problems exoskeleton have been developed which attempt to closely replicate the kinematics of the human arm and form a more intimate contact with limbs of the user. There have been several successful implementations of these devices including:[5-6], the SARCOS Arm Master [3]; and the FREFLEX Master [7].

Unfortunately the SARCOS arm and the FREFLEX still retain the bulky structure of the master slave and remain rigidly fixed to one location. To permit greater freedom of motion 'portable' exoskeletons have been designed where the goal is to ground the exoskeleton on the body of the operator rather than on some external structure.
Devices in this category include: the GLAD-IN-ART Arm Exoskeleton [3]; and the EXOS Force ArmMaster [3].

These systems have increased flexibility but at the expense of increased complexity due to the limited volume and load carrying capacities. This in turn implies high power-to-weight and power-to-volume ratios for the actuating system making their design and specification paramount.

For these new portable exoskeletons it is clear that a key (perhaps the over-ridding requirement) is the provision of an effective actuation system. This system should in addition to the basic power requirements provide ease of use, comfort, sensory accuracy and safety.

In this document we describe the design, construction and testing of a generic light-weight (<2kg) 7 degree of freedom input/feedback system with accurate monitoring of upper limb motion and feedback of forces experienced during contact in a real or/virtual world. The use of novel high power weight pneumatic Muscle Actuators (pMA), will be

0-7803-5841-4/99/$10.00©1999 IEEE

shown to provide low cost, flexibility, portability (both in terms of control platform and physical size), increased safety, and comfort (continuous operations for at least 1 hour). A control algorithm for the system is developed to investigate the effectiveness of the pneumatic force display in creating the illusion of stable virtual surfaces. Experimental results illustrate the interactions between the operator and a virtual wall.

INTERFACE MECHANICAL STRUCTURE

The mechanical arm structure to be used as the basis for this system implementation has 7 DoF corresponding to the natural motion of the human arm from the shoulder to the wrist but excluding the hand. The arm structure has 3 DoF in the shoulder (flexion/extension, abduction-adduction and lateral-medial rotation), 2 DoF at the elbow permitting flexion/extension, pronation-supination of the forearm and 2 DoF at wrist (flexion-extension and abduction-adduction), figure 1.

The arm structure is constructed primarily from aluminium, with joint sections fabricated in steel. The arm is mounted onto a moulded body brace which is light, low cost and comfortable providing a stable platform. The arm and the brace are constructed for use by a 'typical adult' without changes to the set-up, although arm link length changes can easily and quickly be effected, if necessary.

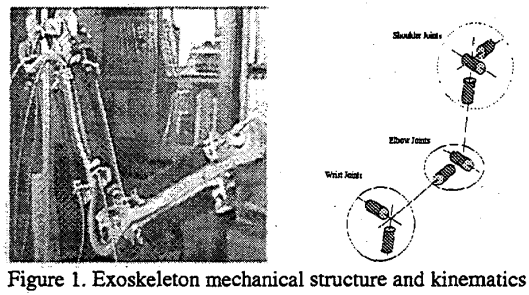

Figure 1. Exoskeleton mechanical structure and kinematics

In principle the exoskeleton duplicates without constraints 90% of the range of the human arm work volume. High linearity sensors were employed to perform the position sensing on the joints.

ACTUATOR DESIGN

The key to the development of a portable exoskeleton is in the design of the actuators. This system will use recently developed pneumatic Muscle Actuators (pMA). PMAs provide a clean, low cost actuation source with a high power/weight ratio and safety due to the inherent compliance. These pneumatic Muscle Actuators (pMA) are constructed as a two-layered cylinder, figure 2. This design has an inner rubber liner, an outer containment layer of braided nylon and endcaps that seal the open ends of the muscle. The complete unit can safely withstand pressures up to 700KPA (7bar), although 600kpa (6bar) is the operating pressure for this system. The detailed construction, operation, and mathematical analysis of these actuators can be found in [9]. The structure of the muscles gives the actuator a number of desirable characteristics [8-10]:

i). This muscle can be made in a range of lengths and diameters with increases in sizes producing increased contractile force.
ii). Actuators have exceptionally high power and force to weight/volume ratios.
iii). The actual achievable displacement (contraction) is dependent on the construction and loading but is typical 30% of the dilated length - this is comparable with the contraction achievable with natural muscle.
iv). Being pneumatic in nature the muscles are highly flexible, soft in contact and have excellent safety potential. This gives a soft actuator option which is again comparable with natural muscle.
v). When compared directly with human muscle the contractile force for a given cross- sectional area of actuator can be over 300N/ cm^2 for the pMA compared to 20-40N/cm^2 for natural muscle.
vi). The actuators can operate safely in aquatic or other liquid environments and are safe in explosive/gaseous states.

The activation of the pMA is reliant on the effective control of the air flow into and from the muscles. This is controlled by MATRIX valves that incorporate 8 controllable ports in a package having dimensions of 45mm x 55mm x 55mm and weighing less than 100g. The valves are controlled using a pulse width modulation regime with a potential pulsing frequency of up to 400Hz, although 40Hz pulses has been found to be adequate for most operations, providing rapid yet smooth motion. Development of an adaptive controller and details of the design of the system can be found in [8-9].

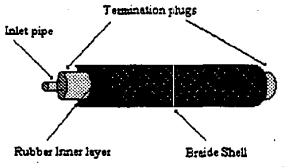

Figure 2. Pneumatic Muscle Actuator Design

ACTUATOR ATTACHMENTS AND JOINT TORQUE CONTROL

Force reflection on the exoskeleton is achieved by producing appropriate antagonistic torques through cables and pulleys driven by the pneumatic actuators. This antagonistic scheme requires two actuators for each joint working in opposition to control the position of the joint and thus, effectively provide constraints in the rotation movements. Since most of joints required a range of rotation in excess of 90°, double groove pulleys have been employed. All joint shafts rotate on bearings to minimise friction. Figure 3 shows the antagonistic torque transmission scheme employed to provide motion constraints to the exoskeleton joints.

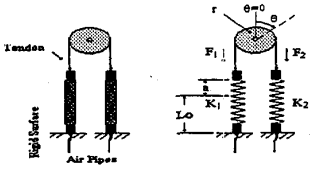

Figure 3. Antagonistic torque transmission scheme and its model.

The muscles used in this project have a diameter of 2cm with an 'at rest' length varying from 15cm to 45cm. Two factors determine the length of the actuator. The first is the required range of motion for the particular joint and the second is the maximum exertable torque required at that joint to constrain the operator's arm. The performance specification for the joints of the human arm are shown in table 1 [11-12], together with the design specification for the FREFLEX (floor mounted exoskeleton) and the achieved joint torque for the pMA exoskeleton.

Joint	Human Isometric Strength	Design Specifications (FREFLEX)	Achieved Joint torque
Shoulder			
Flexion/Extension	110Nm	34Nm	30Nm
Adduction/abduction	125Nm	34Nm	27Nm
Rotation	-	17Nm	6Nm
Elbow			
Flexion/Extension	72.5Nm	17Nm	6Nm
Supination/Pronation	9.1Nm	5.6Nm	5Nm
Wrist			
Flexion/Extension	19.8Nm	2.8Nm	4Nm
Adduction/abduction	20.8Nm	2.8Nm	4Nm

Table 1

The compact actuator structure allows for integration close to their respective powered joints. The wrist actuators (four actuators) and the forearm prono-supination actuator (two actuators) are mounted on the forearm. The elbow actuators (two actuators)and the upper arm rotation actuators (two actuators) are mounted on the upper arm while the shoulder actuators (four actuators) are mounted on the body brace behind the operator's body. Each antagonistic scheme includes a high linearity potentiometer for position sensing and a strain gauge torque sensor. To represent the above antagonistic scheme a model of the pneumatic muscle is required[8-10]. For this system pneumatic actuators are modeled as pure springs with variable stiffness K1, K2. Thus, the forces developed by the actuators for an angle θ are given by

$F_1 = K_1 \cdot (a + r \cdot \theta)$ (1) $F_2 = K_2 \cdot (a - r \cdot \theta)$ (2)

r is the radius of the pulley, θ the rotational angle and a is the dilation of each actuator from the actuator length L_0 when it is fully contracted (figure 4). To achieve the maximum controllable range of motion, a has been set equal to the half of the maximum displacement.

Using an approach similar to that proposed by [10] we consider that the stiffness of each actuator consists of two components one a constant to represent the elasticity of the rubber K_e, figure 4, and one a variable function of the air pressure.

$$K_1 = K_2 = K_p \cdot P + K_e \quad (3)$$

K_p is the stiffness per unit pressure $K_p = \frac{dK}{dP}$ and approximates a constant within the range of the muscle motion as defined in [10].

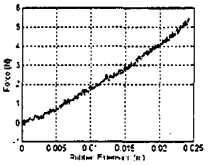

Figure 4: Typical force developed due to the rubber elasticity.

At any time the torque developed at a joint is given by

$$T = (F_2 - F_1) \cdot r \quad (4)$$

It can be seen from (1),(2),(4) that torque can be developed even with zero pressure in the two actuators due to the elasticity of the rubber. One early problems was that the operator could feel these rubber elasticity forces, especially in the free space motions. To overcome the effect and compensate for the undesired forces a joint torque sensor has been incorporated and the closed loop joint torque transmission scheme shown in figure 5 was adopted.

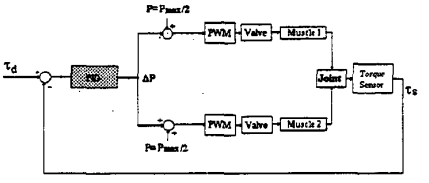

Figure 5: Joint Torque Control scheme

The torque commands for the above torque control loop are generated from a force computation routine, figure 7. The modeling of this force profile which computes the contact forces within the virtual environment will be discussed later. These contact forces are resolved into joint torques (to constrain the motion of the arm) using the transpose Jacobian of the exoskeleton. The torque control loop uses the torque error to calculate the amount of pressure change in the two muscles of the antagonistic pair. The command pressure for the muscles at each cycle are given by

$$P_1 = \frac{P_{\max}}{2} - \Delta P \quad (5) \; P_2 = \frac{P_{\max}}{2} + \Delta P \quad (6)$$

Where ΔP is computed using a PID control law

$$\Delta P = K_p \cdot e + \frac{1}{T_i}\int e + T_d \cdot \dot{e} \quad (7),\; e = \tau_d - \tau_s \quad (8)$$

is the joint torque error, $P_{\max}$ is the maximum pressure within the pneumatic muscle actuators. The exoskeleton joint torque is provided from the integrated strain gauge joint torque sensor. The command pressure for the muscles is converted by the PWM driver into a PWM signal which drives the solenoid valves to control the pressure in the pneumatic actuators. The duty cycle of the PWM signal is directly proportional to the pressure command. The above closed loop joint control scheme[13] compensates not only the actuator

shortcomings such as actuator elasticity but also for joint friction etc and enhances the quality of the response of the antagonistic scheme to torque commands.

MODELING OF THE VIRTUAL CONTACT FORCES

The human arm can be divided into three zones (upper arm, forearm and palm). Realistic physical interaction demands that collisions with these links be accurately detected and contacts simulated effectively. Should any of the above three zones collide with a virtual object the force feedback is accomplished by generating a force to constrain the motion in such a way as to create the illusion of interaction with a real object. This virtual force is defined to be zero if the virtual arm is in free space. The nature of the contact forces between the virtual manipulator and its environment depends on the particular application. For example, the contact of the virtual arm and a stiff virtual object like a metal plate represents a spring-like phenomenon, with the force being dependent on the displacement of the spring from its resting position. When the manipulator moves in a viscous environment the interaction of the manipulator with the environment can be modeled as a damper with the force being dependent on the velocity. Considering the above, a model for a contact between the virtual manipulator and the environment can best be illustrated with a coefficient B and a spring with stiffness K. Figure 6 illustrates this approach.

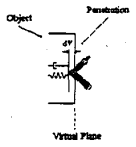

Figure 6: Model of the virtual wall

In general this virtual model of a stiff spring-damper system is the most commonly adopted approach and implementations of such a contact model have been widely used in various haptic interfaces [14-16]. The damping term is usually applied to prevent oscillations caused by the high stiffness. Similar models can be applied to all rotational screw motion. The contact is modeled by an equivalent rotational dynamic equation which contains the torsional spring and damping coefficients K, B respectively.

To provide a simple model for test purposes a virtual environment has been created consisting of some virtual planes (walls) and a virtual arm with the kinematics of the operator's arm. The collision detection algorithm identifies contact between the virtual environment and one of the three links of the simulated arm (upperarm, forearm, palm). This simulated arm is composed of a series of polygons to ensure that the contact point can be accurately focussed on a specific section on the arm. Each of these polygons can be considered to be an entity in its own right and checks can be made on the intersection of each polygon with the virtual walls. This permits accurate modeling of the impact area and the forces that must be imparted to the arm to create the most realistic impression of arm/object contact. Every virtual object in the virtual environment can be constructed a network of interlinked virtual planes. These virtual planes are defined by the following equation.

$$a \cdot x + \beta \cdot y + \gamma \cdot z + \delta = 0 \qquad (9)$$

Where the vector (a, β, γ) is the unit vector normal to the virtual plane and specifies its orientation. The variables (x, y, z) represent the coordinates on the plane. When a collision between a polygon of the virtual arm and a plane of the virtual object is detected the orientation of the intersected plane, the attributes of the plane (stiffness, damping) and the centre of gravity of the intersecting polygon are used by the force computation routine to determine the resultant forces to be reflected to the exoskeletal arm.

After the collision, the penetration depth of the arm polygon into the plane is calculated according to:

$$d\psi = \frac{\left| a \cdot x_p + \beta \cdot y_p + \gamma \cdot z_p \right|}{\sqrt{a^2 + \beta^2 + \gamma^2}} \qquad (10)$$

The position of the centre of gravity of the polygon (x_p, y_p, z_p) is computed using the forward kinematics. The penetration depth together with the attributes of the intersected plane are used by the force computation routine to calculate the 3 dof force intersection vector.

A similar approach is used for the rotational 'screw' motions. The torsional penetration is calculated from the twist of the intersected frame after the moment of contact. This torsional penetration is used to calculate the 3 dof torque intersection vector. The 6 dof simulated force/torque vector is then resolved into joint torque using the exoskeleton Jacobian. The Jacobian used to resolve the simulated force/torque into joint torques is dependant on the polygon on the virtual arm which is in collision with the virtual object. If the collision is with a polygon in the upper arm, the reflected forces are generated by the 3 dof of the shoulder joint. A 6x3 Jacobian is used to map the collision forces into joint torques. The vector of the desired torques in joint space τ_d is given by:

$$\tau_d = J^T{}_{upperarm}(\theta) \cdot \begin{bmatrix} F \\ M \end{bmatrix} \qquad (11)$$

F, M : describe the forces and moments acting at the contact point.

τ_d : vector of the joint torques.

If the collision is with a polygon forming part of the forearm, the reflected forces are generated by the 3 dof of the shoulder and the 2dof of the elbow. A 6x5 Jacobian is used to map the collision forces into joint torques. In this instance the vector of the desired torques in joint space τ_d is

$$\tau_d = J^T{}_{lowerarm}(\theta) \cdot \begin{bmatrix} F \\ M \end{bmatrix} \quad (12)$$

Finally, if the collision is with a polygon in the hand or a tool held in the hand, then the forces are generated by the 7 dof of the whole arm. A 6x7 Jacobian is used to map the collision forces into joint torques. The vector of the desired torques in this case is given by:

$$\tau_d = J^T{}_{palm/tool}(\theta) \cdot \begin{bmatrix} F \\ M \end{bmatrix} \quad (13)$$

In case of multiple contact points only the polygon which is furthest down the kinematic chain of the exoskeleton is considered. The joint torques computed above are used to provide the input τ_d to drive the joint torque control scheme previously described, figure 5. This enables the exoskeleton to simulate contact phenomena. The overall control scheme of this system is shown in figure 7.

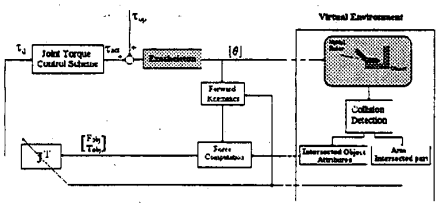

Figure 7: Control scheme of the overall system.

Where τ_{op} represents the operator torque which is actually the force felt by the operator.

VIRTUAL REALITY SYSTEM

From the first stages of the implementation of the system it was clear that satisfying the force feedback and graphics requirements and achieving adequate performance (15 frames/s visual response and 120Hz in the haptic control scheme) would require a distributed interactive simulation. This is because the control update rate of the force reflection system was difficult while trying to generate real time 3D graphics. The hardware of the virtual reality system is shown in figure 8. It consists of the pMA powered exoskeleton, a Haptic PC and a Silicon Graphics machine. The Haptic PC provides I/O control of the force reflection system and runs the force reflection controller. The CPU of this computer is a Pentium II(266MHz) with 64MB RAM and 8MB VRAM.The Silicon Graphics O2 machine generates real time images of the virtual world and performs the collision detection between the virtual arm and the virtual object within the virtual world. This is a "Window on World" system that uses a conventional computer monitor to display the virtual world. The virtual world was developed on the Silicon Graphics using the commercial VR packet "WorldToolKit". The Display machine communicates with the Haptic PC through an RS232 serial link at 57600bps. The communication loop between the two machines is performed at an update frequency of 25Hz while the control update rate at the Haptic PC is 120Hz. This is proved to be adequate givingrobust reliable operation. In tests this proved capable of providing a stable robust and reliable system performance.

Figure 8: Virtual reality system

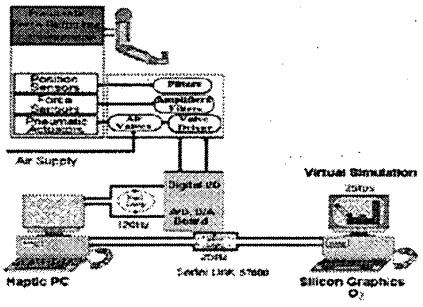

VIRTUAL WALL INTERACTIONS: EXPERIMENTAL RESULTS

To test the system a number of experiments have been performed using the controller shown in figure 7. The experiment was implemented as a sampled-data system using the configuration shown in figure 9. The Haptic PC performed the position sampling and computed the reaction forces while the Silicon Graphics updated the position of the virtual arm according to the movements of the operator's arm and performed the collision detection, figure 9. The sampling interval and the period of the pulse width modulator are 8ms while an operating pressure of 600KPa (6bar) was used. Experiments were conducted to test the following effects.

i) Unrestricted free space motion
ii) Contact testing with a virtual object
iii)Tests of contact characteristics with walls having different properties

Figure 9: Operator interacting with a virtual object

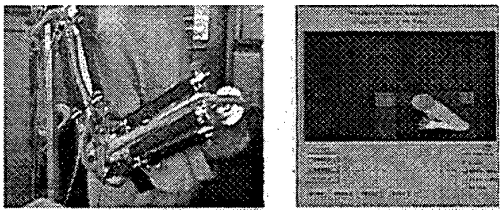

In experiment 1 the operator was asked to move his arm in the free region around the virtual wall without touching the wall. Although the mechanism has no gravity compensation the lightness of the system make it be quite comfortable for long period operations (at least 1 hour). The operators reported the presence of no detectable forces giving a realistic sensation of free space and no tiring.

In experiment 2 the operator was asked to maneuver the exoskeleton to detect a virtual table. This surface was located at the $x = 0.15$ plane. Figure 11a shows motion of the operator's arm in the vertical (x-direction) prior to contact and at the contact instant. Figure 11b shows the forces developed during the contact. From these results it can be seen that free space motion is unrestricted (as required) but at the $x = 0.15$ plane, motion is constrained. At this point the force recorded rises rapidly preventing penetration of the operator's arm into the virtual table. The results shows that the table position is located at $x = 0.164$. This is due to the

spring constant set for the table. It was reported (by operators) that the stiffness of this virtual table does not 'feel' like a hard contact expected from a fist or knuckle touching a solid object such as wood or metal, but is rather more like touching a hard object with a fleshy arm surface. Since all arm surfaces have this 'fleshy' covering, the operators felt the general sensations qualitatively very close to natural contact. From the results shown in figures 10, it is clear that virtual contact produces a stable interaction. For the modeled table the spring and damping constants were: K=600N/m, B=40Nsec/m

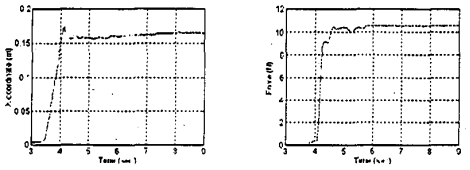

(a) (b)

Figure 10. Interaction with a virtual table.

In experiment 3 virtual interactions with walls having different properties in terms of stiffness and damping were performed. Figures 11a, 11b shows some typical results obtained during the interactions. In Figure 11a an interaction with a wall with an increased stiffness and damping factor (K=1000N/m and B=160Nsec/m) is illustrated. Due to differentiation noise and the high damping in this instance, small oscillations are induced which can be felt by the operator as small vibrations. Further work is under way to investigate the effectiveness of the addition of a low pass filter as proposed by [17] in order to filter the velocity estimation and increase the velocity resolution. Figure 11b presents the results of the interaction with a very stiff wall but having the damping returned to it original value (K=1400N/m and B=40Nsec/m). An increased bouncing instability at the moment of contact was noted which is primarily due to the large virtual stiffness. The operators reported that this increased instability can easily be felt at the moment of contact but fortunately decays rapidly resulting in a subsequently stable wall.Comparing the steady state penetration of the walls in figures 10 and 11 it is clear that the penetration depth at steady state is reduced as the stiffness increases.

K=1000N/m K=1400N/m
B=160Nsec/m B=40Nsec/m

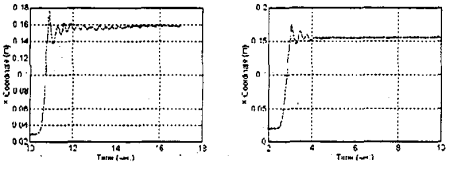

(a) (b)

Figure 11: (a) Interaction with a stiff and high damped wall , (b) Interaction with a very stiff wall

CONCLUSION/FURTHER WORK

Virtual reality, training and hazardous environment task simulations can be enhanced by the addition of force feedback. This work has shown the development of a full arm exoskeleton force display which is capable of creating the illusion of contacts between the operator arm and virtual surfaces. Along with its effectiveness to replicate contact forces, the system had a specific goal of portable, user friendly operation, and was designed to meet the specifications of light-weight and safety which form a dominant requirement for the widespread use of the force feedback. To meet the above specifications novel pneumatic Muscle Actuators were employed to power each of the 7 exoskeleton joints. This type of actuation has an excellent power/weight ratio and inherent safety. Experimental tests have been performed giving encouraging results about the feasibility of the interface to replicate contact forces. Future work will include:

i) the integration of the arm force display with a currently under construction pMA powered hand display for monitoring of finger motions and replication of contact forces at the level of the hand. This will enable control of remote/virtual manipulators with dextrous hands.

ii) the use of the system to execute more difficult tasks such as virtual peg insertion, virtual weight lifting etc.

iii) the development of a training simulation to investigate the use of the pMA exoskeleton display in training and hazardous environment task applications.

iv) the use of the system for medical applications, especially as an upper limp motion assisting system[16] or as a treatment system for recovering from upper limb injuries.

REFERENCES

[1] T.B.Sheridan, "Tele-robotics, Automation and Human Supervisory Control", MIT Press, 1992.

[2] M. Minsky, Ming Ouh-young, O. Steele, F.P.Brooks, Jr.M. Behensky , *"Feeling and seeing, Issues in force display"*, Computer Graphics, Vol 24, no 2, pp 235-243, 1990

[3] G.C.Burdea,"Force and touch Feedback for Virtual Reality",John Wiley & Sons,Inc, 1996.

[4] S.Tachi, H. Arai, T. Maedo, E.Oyama, N Tsunemoto, and Y. Inoue, *"Tele-existance in Real World and Virtual World"*, 5th Intl Conf. on Advanced Robotics, ICAR '91, pp.193-98, Pisa, Italy, 1991.

[5] Sooyong Lee, Sangmin Park, Munsang Kim, Chong-Won Lee, *"Design of a force Reflecting Master Arm and Master Hand using Pneumatic Actuators"*, Procedings of the 1998 IEEE International Conference on Robotics & Automation, Belgium May 1998

[6] Kiyoshi Nagai, Isao Nakanishi, Hideo Hanafusa, Sadao Kawamura, Masaaki MakiKawa, Noriyuki Tejima,*"Development of an 8 DOF Robotic Orthosis for assisting Human Upper Limp Motion"* ,Proceedings of the 1998 IEEE International Conference on Robotics & Automation, Leuven, Belgium May 1998.

[7] Burke, J., 1992, *"Exoskeleton Master Arm, Wrist and Effector Controller with Force Reflecting Telepresence"*,Technical Report AL/CF-TR-1994-0146,Odentics Inc.,Anaheim CA, 104pp., December.

[8]D.G.Caldwell,G.A.Medrano-Cerda,M.Goodwin *"Characteristics and Adaptive Control of Pneumatic Muscle Actuators for a Robotic Elbow"*,Proceedings of 1994 IEEE International Conference on Robotics and Automation, pp 3558-3563,San Diego,California,May 8-13.

[9] D.G.Caldwell, G.A.Medrano-Cerda, and M.J.Goodwin, *"Control of Pneumatic Muscle Actuators"*, IEEE Control Systems Journal, Vol.15, no.1, pp.40-48, Feb. 1995.

[10] Ching-Ping Chou and Blake Hannaford, *"Measurement and Modeling of McKibben Pneumatic Artificial Muscles"*, IEEE

TRANSACTIONS On Robotics and Automation Vol 12, No 1,February 1996.

[11] K. N. An, L. J. Askew, E. Y. Chao, *"Biomechanics and functional assessment of upper extremities"*, Trends in Ergonomics/Human Factors III, Elsevier Science Publishers B.V. (North-Holland), 1986

[12] Human Engineering Guide to equipment design, American Institutes for Research Washington D.C. 1972

[13] Darwin G.Caldwell, N.Tsagarakis, G.A.Medrano-Cerda, J.Schofield, D.Pye and S.Brown, *"Development of Pneumatic Muscle Actuators for B30 Retrieval Operations"*,1999 IEEE International Conference on Robotics and Automation (submitted)

[14] T.H. Massie and J.K. Salisbury,*"The PHANToM haptic interface: A device for probing virtual objects"*, ASME Winter Annual Meeting, vol 1, pp. 295-299,1994

[15] J.E. Colgate, P.E. Grafing, M. C. Stanley, and G. Schenkel,*"Implementation of Stiff Virtual Walls in Force-Reflecting Interfaces"*, Proceedings of the IEEE Virtual Reality Annual International Symposium (VRAIS), IEEE, New York , pp 202-208, September 1993.

[16] M. Ching and D. W.L Wang,*"A Five-bar-linkage Force Reflecting Interface for Virtual Reality System"*, Proceedings of the 1997 IEEE International Conference on Robotics and Automation, Albuquerque,New Mexico-April 1997.

[17] E.Colgate and M. Brown, 1994, "Factors Affecting the Z-Width of a Haptic Display",Proceedings of 1994 IEEE International Conference on Robotics and Automation, pp 3205-3210, San Diego,California ,May.